PROCEEDINGS OF SCIENCE

Ultra-high energy muons in radio neutrino detectors

Lilly Pyras,[a,b,*] **Christian Glaser,**[c] **Steffen Hallmann**[a] **and Anna Nelles**[a,b]

[a] *Deutsches Elektronen-Synchrotron DESY, Platanenallee 6, 15738 Zeuthen, Germany*

[b] *Erlangen Center for Astroparticle Physics (ECAP), Friedrich-Alexander-Universität Erlangen-Nürnberg, Nikolaus-Fiebiger-Straße 2, 91058 Erlangen, Germany*

[c] *Uppsala University, Department of Physics and Astronomy, Uppsala SE-752 37, Sweden*

E-mail: lilly.pyras@desy.de, christian.glaser@physics.uu.se, steffen.hallmann@desy.de, anna.nelles@desy.de

With the prospect of large volume radio neutrino detectors such as RNO-G and IceCube-Gen2, measuring neutrinos above PeV energies is within reach. At these energies, atmospheric muons stemming from cosmic ray air showers represent a rare background: They penetrate the ice and can mimic the interaction of a neutrino through catastrophic energy losses. Due to both limited experimental measurements and limited modeling in hadronic interaction models, the expected event rate is subject to large uncertainties. In this study, we predict rates and associated uncertainties and evaluate mitigation strategies, such as parent air shower detection.

The 38th International Cosmic Ray Conference (ICRC2023)
26 July – 3 August, 2023
Nagoya, Japan

*Speaker

PoS(ICRC2023)1076

1. Introduction

With large volume radio detectors such as RNO-G and IceCube-Gen2 the detection of an astrophysical neutrino above 10 PeV is within reach. Because the flux predictions vary widely, a good understanding of rares backgrounds is necessary for these discovery experiments. The radio signal to be detected is generated by the particle cascade following a neutrino interaction in ice. The build-up of a net negative charge at the shower front leads to the emission of coherent radiation, the Askaryan emission [1]. Due to a Cherenkov-like effect, the emission is strongest at the Cherenkov angle (~56° in ice). The signal amplitude at a given observer distance scales linearly with the shower energy [2] and is typically visible above the thermal noise at 5 PeV to 10 PeV [3]. Due to this emission mechanism, any particle cascade induced in the ice with the necessary energy deposit creates a detectable signal, independent of its parent particle. This means that also high-energy muons stemming from air showers could act as a background in neutrino detectors whenever they initiate a shower [4]. The predicted muon event rate depends on the hadronic interaction models and the cosmic ray composition, which are not-well determined, especially above PeV energies. These proceedings summarize and add to what has been shown in [5].

2. Muon flux predictions

Atmospheric muons are generated in extensive air showers when a cosmic ray nucleon interacts with an air nucleus and produces short-lived intermediate particles, mostly pions (the lightest known meson) and a few heavier particles with shorter life times, such as kaons, D-mesons, etc. The highest energy muons are generated within the first interactions, since which each generation the energy is distributed equally between the daughter particles and less energy per muon is available [6]. The relevant cosmic rays are protons, since they contain the kinetic energy in one nucleon rather than iron which divides the energy to 56 nucleons. Consequently, one has to concentrate on the highest energy interactions to study the relevant muon background. Unfortunately, these interactions are far outside of the energy regime currently observable at accelerators, which makes far-reaching extrapolations necessary.

The *conventional component* of the muon flux includes muons through the decay of short-lived mesons, namely charged pions and kaons [7]. At very high energies the Lorentz time dilatation increases the decay length of pions and kaons to a multiple of their interaction length (ℓ_{int}) in air, making it more likely that they will interact and lose energy before they can decay. The contribution of particles with a shorter lifetime τ then becomes dominant. Due to their almost immediate decay the contribution of short-lived hadrons with $c\tau \ll \ell_{\text{int}}$ is called *prompt flux* and dominates above 10^6 GeV. The prompt flux can be divided into four components: the decay of charmed hadrons ($D^0, D^+, D_s^+, \Lambda_c^+, \Omega_c^0$ and their antiparticles) [8], the decay of bottom hadrons ($B^0, B^+, B_s^+, B_c^+, \Lambda_b^0, \Xi_b^0, \Xi_b^+$) [9], the decay of unflavored mesons ($\eta, \eta', \rho^0, \omega, \phi$) [9] and photo-conversion into a muon pair ($\gamma Z \to \mu^+\mu^- Z$) e.g. Bethe-Heitler process, Drell-Yan processes [9] and photo-conversion into a vector meson (including J/Ψ) decaying into muons [10, 11].

Taking into account these different sources, the atmospheric muon flux can then be expressed as the sum of five components:

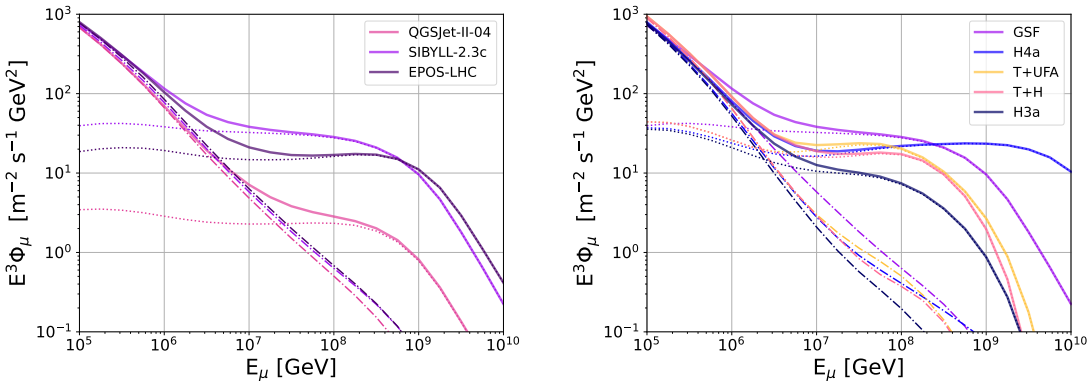

Figure 1: Simulated muon flux as function of muon energy for different hadronic interaction models (left) and cosmic-ray composition models (right). Shown are the predictions for QGSJET-II.04 [14], SIBYLL-2.3C [12], and EPOS-LHC [13] for the Global Spline Fit (GSF) [15] cosmic ray composition. Dashed lines represent the prompt muon flux and dash-dotted is conventional muon flux. The right shows different cosmic ray composition models using SIBYLL-2.3C: GSF [15], HillasGaisser (H4a) [16], T+UFA, [17, 18], T+H [17, 19] and HillasGaisser (H3a) [16].

$$\phi_\mu(E,\theta) = \phi_\mu^{\text{conv}}(E,\theta) + \phi_\mu^{\text{charm}}(E,\theta) + \phi_\mu^{\text{unflav}}(E,\theta) + \phi_\mu^{\gamma}(E,\theta) + \phi_\mu^{\text{bottom}}(E,\theta). \quad (1)$$

Different hadronic interaction models are available, which take different production channels into account. SIBYLL-2.3C [12] is the most complete models, including muons from charm decay, unflavoured mesons and J/Ψ but neglect photo-conversion and B-mesons. EPOS-LHC [13] includes only unflavoured mesons, the prompt component in QGSJET-II.04 [14] arises from η decay. The resulting difference in the muon flux is shown in Fig. 1 left.

The cosmic ray spectrum covers several decades of energy up to 10^{11} GeV, including particles from galactic and extra-galactic origin. Just below the so-called ankle at 8×10^9 GeV, the transition region from galactic to extra-galactic cosmic rays is expected [20, 21], with different theoretical models interpreting features differently.

Measurements of the cosmic ray composition above a few 10^5 GeV suffer from the uncertainties in the hadronic interaction models, since the composition has to be inferred from shower parameters such as the position of the shower maximum X_{max}, which provides composition models with much room for interpretation. Since the ultra-high energy muon flux directly depends on the cosmic ray composition, these uncertainties propagate into the muon flux predictions. Different models have been investigated to study the uncertainty stemming from this aspect. We also combine models to study the influence of galactic and extra-galactic components. This is done to show the spread in models, rather than choosing one over the other. The well-known Hillas Gaisser models are theoretical simplifications for extreme scenarios: a heavy composition after the ankle (H3a) [16] and a proton-rich composition (H4a) [16]. This is contrasted by the Global Spline Fit (GSF) [15], a data-driven parameterization that considers measurements of more than ten experiments and provides uncertainties at each energy. GSF is agnostic to theoretical models explaining the

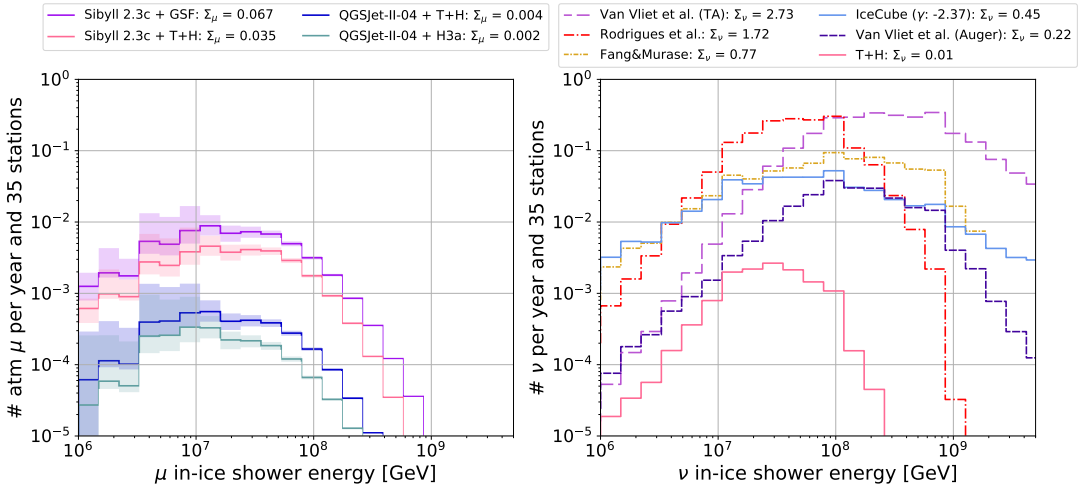

Figure 2: Left: Expected muon event rate for a 2.5σ trigger in the deep component evaluating four extreme scenarios in combining hadronic interaction model and cosmic ray composition as stated in the label. Right: Various predictions for an expected neutrino event rate with a 2.5σ trigger in the deep component, including cosmogenic neutrinos (TA [22–24], Auger [24], T+H [17, 19]) and neutrinos from sources (Fang and Murase [25], Rodrigues et al. [26])

derived composition in terms of sources and propagation. Thoudam et al. [17] published different theory-driven cosmic ray spectra up to EeV energies. In the following, their prediction for cosmic rays stemming from Supernova remnants (SNR-CR) and Wolf-Rayet stars (WR-CR) is used as a galactic component, labeled *T*, and are combined with different extra-galactic components. The UFA model by [18] predicts a strong pure-proton component concentrated only about one order of magnitude in energy below the ankle. For our combination into the T+UFA model the results are optimized for a pure nitrogen galactic composition, which matches the predicted composition for WR-CR [17]. The extra-galactic component of Heinze et al. [19] is based on a framework in which an ensemble of generalized ultra high energy cosmic ray accelerators is characterized by an universal spectral index (equal for all injection species), a maximal rigidity, and the normalizations for five nuclear element groups. The source evolution is included as an additional free parameter. This allows for a parameter scan with a best fit result. The composition used in this paper is obtained by a fit to the Auger data from 2019. The resulting muon fluxes are shown on the right in Fig. 1 for Sibyll-2.3c as hadronic interaction model.

3. Signature in radio detectors

Simulations were performed for an RNO-G like detector array with 35 stations. Each station is comprised of a dipole antenna (Vpol) located at a depth of −100 m in the ice (*deep component*), and three log-periodic dipole antennas (LPDA) pointing straight down located at the surface (*shallow component*). The simulation framework is detailed in [5]. The relevant quantity to radio detectors is the energy which is transferred into the particle shower, which is usually a factor 10 lower than the particle energy. Fig. 2 left shows the expected muon rate for a combination of extreme scenarios in terms of shower energy. The hadronic interaction model Sibyll-2.3c combined with the GSF

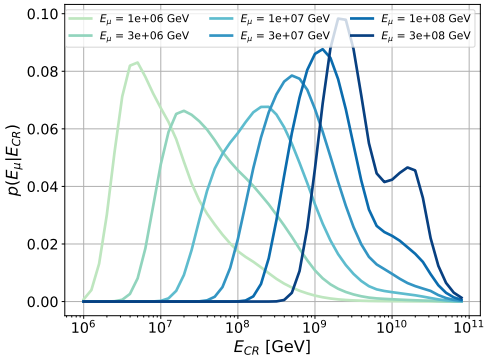

Figure 3: Relation of muon energy to parent cosmic ray energy. The distributions show the probability that a muon with a given energy (color code) stems from a cosmic ray with an energy as indicated in the x-axis.

cosmic ray composition yields 0.07 muons per year and 35 stations, changing the cosmic ray model to a heavier composition reduces the muon number by half. Choosing QGSJET-II.04 as generator, results in almost no muons trigger. This is expected, since QGSJET-II.04 includes less muon production channels, which are especially relevant at the highest energies. The differences using SIBYLL-2.3C and GSF, and T+H respectively are therefore likely a more complete and conservative estimate for the uncertainties of the muon event rate, reducing the uncertainty budget to a factor of 2, keeping in mind that SIBYLL-2.3C still does not model all components of the muon production. Fig. 2 right shows the expected neutrino rate for the same detector and various models, including cosmogenic neutrinos and neutrinos from sources. Most muons are expected between 10^7 GeV to 10^8 GeV, towards higher energy their rate falls steeply. Above 10^8 GeV all shown neutrino predictions are higher than the muon expectation, which provides an avenue towards a possible analysis cut at high energies.

4. Muon and parent air shower

One possibility to distinguish a muon event from a neutrino induce shower is to detected the parent cosmic ray of the muon. Since radio detectors like RNO-G also consist of upward facing antennas, air shower detection is already integrated in the system. To quantify the veto efficiency one needs a relation between cosmic ray energy and muon energy. Since the ultra-high energy muons are boosted along the shower axis, the arrival direction can assumed to be the same. Fig. 3 shows a probability distribution that a muon with a certain energy originates from certain cosmic ray. Most likely a muon stems from a cosmic ray that has an energy a decade higher than the muon itself. The relation is retrieved by simulating air showers with a certain primary and scaling the muon content according to the cosmic ray composition, as detailed in [5]. To calculate the veto on event basis, for each muon an air shower simulated with textscCORSIKA [27] and the matching arrival direction is placed inside the detector array according to the muon position. The resulting radio signal is simulated with CORSIKAs radio extension CoREAS [28] and then folded with the detector response using NuRadioReco [29]. Since the amplitude of the air shower signal scales linearly with the cosmic ray energy [30] it can now be calculated, which air shower energy is necessary to exceed a simple $2.5\sigma_{\text{noise}}$ trigger threshold in an upward-pointing shallow LPDA

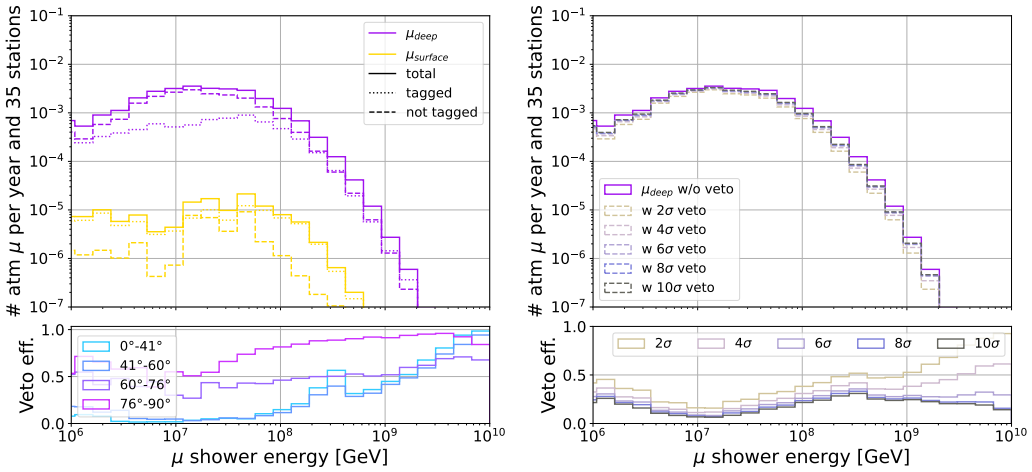

Figure 4: Cosmic ray veto for muon events using SIBYLL-2.3C as hadronic interaction model and GSF as cosmic ray composition. Left: Expected event rate for all muon events (solid line), muons with measured parent air shower (dotted) and muons without measured air shower (dashed). The color code indicates in which detector component the muon was measured. The lower panel shows the veto efficiency for different zenith arrival direction as indicated in the label. Right: The color code indicated different trigger thresholds for the cosmic ray veto. The lower panel shows the veto efficiency.

antenna and hence veto the muon event. In the last step, the probability that a muon event stems from an air shower with an energy higher than the trigger threshold energy is calculated and assigned to that muon. Combined with the predicted muon flux, the number of muons that can be vetoed by detecting the parent cosmic ray can be calculated. Fig. 4 left shows a veto efficiency close to 100% for muon energies > 10^9 GeV. Muons originating from inclined air showers are more likely to be vetoed since the radio signal for inclined air showers covers a larger area but becomes fainter at the same time. Therefore the veto efficiency increases with higher zenith angles only for higher energies. Fig. 4 right shows the depends on the trigger threshold. A lower threshold improve the veto, especially at the highest energies. Those event, with a cosmic ray energy around 10^{11} GeV are, however, very rare. To improve the veto efficiency, a denser array of antennas would be needed. However, such an in-fill array would have to have a spacing of $O(100)$m, making it too dense to be feasibly installed.

To get a better understanding of the event geometries the station multiplicity and the relation of cosmic ray trigger to muon trigger have been investigated. Fig. 5 left shows, that almost all deep muons trigger only one station. This is expected, as the station spacing of 1.25 km has been optimized to cover the largest possible volume, rather then focus on multiple triggers. Most air showers do not trigger in the vicinity of the muon trigger (85%), but have to self-trigger another station, see Fig. 5 right. This is especially true for inclined air showers, where the muon can travel up to 4 km in the ice before inducing a visible radio signal. For ~10% of the deep muon events, the cosmic ray triggers the same station, which would allow for a sub-threshold search. This behavior is similar for all triggers, since the detection location is determined mostly three factors: the travel distance of the muon, before it induces an visible shower (I), the cherenkov cone (II), where the radio signal is strongest and therefore measurable (opening angle of 56°). Plus, the radio signal gets bend down while propagation through the ice. This is a consequence of the changing refractive

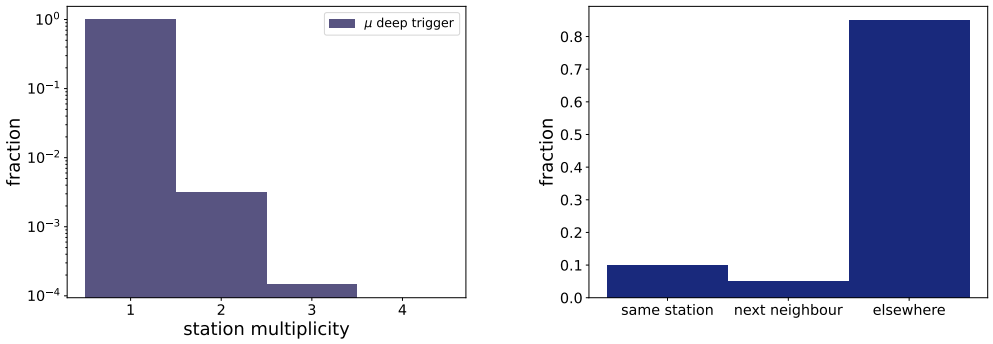

Figure 5: Event geometry inside the array. Right: Fraction of the muon events where the deep trigger triggers one, two or three different stations of the array. Left: Relation of cosmic ray triggered station to deep muon triggered station. For ∼10% of the muon event the cosmic ray trigger occurs in the same station as the deep muon trigger, in ∼5% of the cases the cosmic ray trigger occurs in the nearest neighboring station, the rest of the cosmic rays is expected to trigger elsewhere in the array.

index (III). Therefore, most events who have muon and cosmic ray trigger in the same station arrive at an zenith angle of $\theta \approx 50°$. Possible implications for the hardware regarding the time difference are described in [5].

5. Conclusion

We showed that atmospheric muons at PeV energies and beyond are a non-negligible background to radio neutrino detectors in ice. The ultra-high energy muon flux is highly dependent on hadronic interaction models and the proton fraction of cosmic ray composition. Sibyll-2.3c currently provides the most complete hadronic interaction model for these high energies, since it considers the conventional component, the contribution from charmed hadrons and muons from unflavored mesons, neglecting only the subdominant contributing from B-mesons and photo-conversion into muon pairs. The cosmic ray composition influences the muon rate mostly through the parameter of the proton fraction. Changing from a proton-rich to a proton-poor model, yields a difference of a factor of two in flux prediction. An RNO-G like detector with 35 stations will observe about 0.07 muons per year, using the Sibyll-2.3c prediction and a 2.5σ-threshold. These numbers should be compared to the very uncertain flux predictions for neutrinos, which are ranging from 2.7 neutrinos to 0.01 neutrinos per year in RNO-G.

A possible mitigation strategy is to detect cosmic rays and thereby identify muon events: if the parent air shower of the muon can be detected, it provides a signature unique to muon events. The efficiency of this mechanism is energy and arrival direction dependent with good efficiency for a zenith arrival direction more inclined than 55° zenith and muon energies above 10^9 GeV. It is, however, likely that neutrinos and muons show a different energy spectrum. The muon flux will likely not be measurable above 10^9 GeV shower energy, already being smaller than most neutrino fluxes at 10^8 GeV shower energy. The obtainable resolution of the shower energy of radio neutrino detectors is expected to be better than a factor of two [3], which seems sufficient to assign a significant signalness probability for high energy events. Combined with an air shower veto, which

is most efficient at high energies, this should allow for a relatively background-free neutrino shower detection above 10^8 GeV.

References

[1] G. A. Askar'yan *Zh. Eksp. Teor. Fiz.* **41** (1961) 616–618.
[2] E. Zas, F. Halzen, and T. Stanev *Phys. Rev. D* **45** (1992) 362–376.
[3] **RNO-G** Collaboration, J. A. Aguilar *et al. Eur. Phys. J. C* **82** no. 2, (2022) 147.
[4] D. García-Fernández, A. Nelles, and C. Glaser *Phys. Rev. D* **102** no. 8, (2020) 083011.
[5] L. Pyras, C. Glaser, S. Hallmann, and A. Nelles *under review JCAP, [arXiv: 2307.04736]* (7, 2023) .
[6] J. Matthews *Astropart. Phys.* **22** (2005) 387–397.
[7] R. Engel, D. Heck, and T. Pierog *Ann. Rev. Nucl. Part. Sci.* **61** (2011) 467–489.
[8] J. I. Illana, P. Lipari, M. Masip, and D. Meloni *Astropart. Phys.* **34** (2011) 663–673.
[9] J. I. Illana, M. Masip, and D. Meloni *JCAP* **09** (2009) 008.
[10] L. V. Volkova *Phys. Atom. Nucl.* **74** (2011) 318–323.
[11] C. Gámez, M. Gutiérrez, J. S. Martínez, and M. Masip *JCAP* **01** (2020) 057.
[12] F. Riehn, H. P. Dembinski, R. Engel, A. Fedynitch, T. K. Gaisser, and T. Stanev *PoS* **ICRC2017** (2018) 301.
[13] T. Pierog, I. Karpenko, J. M. Katzy, E. Yatsenko, and K. Werner *Phys. Rev. C* **92** no. 3, (2015) 034906.
[14] S. Ostapchenko *Phys. Rev. D* **83** (2011) 014018.
[15] H. P. Dembinski, R. Engel, A. Fedynitch, T. Gaisser, F. Riehn, and T. Stanev *PoS* **ICRC2017** (2018) 533.
[16] T. K. Gaisser *Astroparticle Physics* **35** no. 12, (Jul, 2012) 801–806.
[17] S. Thoudam *et al. Astron. Astrophys.* **595** (2016) A33.
[18] M. Unger, G. R. Farrar, and L. A. Anchordoqui *Phys. Rev. D* **92** no. 12, (2015) 123001.
[19] J. Heinze, A. Fedynitch, D. Boncioli, and W. Winter *The Astrophysical Journal* **873** no. 1, (Mar, 2019) 88.
[20] J. P. Rachen, T. Stanev, and P. L. Biermann *Astron. Astrophys.* **273** (1993) 377.
[21] V. S. Berezinsky, S. I. Grigoreva, and B. I. Hnatyk *Nucl. Phys. B Proc. Suppl.* **151** (2006) 497–500.
[22] **ARIANNA** Collaboration, A. Anker *et al. [arXiv: 2004.09841]* (4, 2020) .
[23] **Telescope Array** Collaboration, D. Bergman *PoS* **ICRC2021** (2021) 338.
[24] A. van Vliet, R. Alves Batista, and J. R. Hörandel *Phys. Rev. D* **100** no. 2, (2019) 021302.
[25] K. Fang and K. Murase *Nature Phys.* **14** no. 4, (2018) 396–398.
[26] X. Rodrigues, J. Heinze, A. Palladino, A. van Vliet, and W. Winter *Phys. Rev. Lett.* **126** no. 19, (2021) 191101.
[27] D. Heck, J. Knapp, J. N. Capdevielle, G. Schatz, and T. Thouw, "CORSIKA: A Monte Carlo code to simulate extensive air showers." `http://bibliothek.fzk.de/zb/berichte/FZKA6019.pdf`, 2, 1998.
[28] T. Huege, M. Ludwig, and C. W. James *AIP Conf. Proc.* **1535** no. 1, (2013) 128.
[29] C. Glaser, A. Nelles, I. Plaisier, C. Welling, S. W. Barwick, D. García-Fernández, G. Gaswint, R. Lahmann, and C. Persichilli *The European Physical Journal C* **79** no. 6, (Jun, 2019) .
[30] **Pierre Auger** Collaboration, A. Aab *et al. Phys. Rev. Lett.* **116** no. 24, (2016) 241101.